# Minimum-dissipation models for large-eddy simulation

Cite as: Phys. Fluids **27**, 085107 (2015); https://doi.org/10.1063/1.4928700
Submitted: 30 April 2015 . Accepted: 05 August 2015 . Published Online: 19 August 2015

Wybe Rozema, Hyun J. Bae, Parviz Moin, and Roel Verstappen

PHYSICS OF FLUIDS **27**, 085107 (2015)

# Minimum-dissipation models for large-eddy simulation

Wybe Rozema,[1,2,a)] Hyun J. Bae,[3] Parviz Moin,[3] and Roel Verstappen[1]
[1]*Johann Bernoulli Institute for Mathematics and Computer Science, University of Groningen, Nijenborgh 9, 9747 AG Groningen, The Netherlands*
[2]*National Aerospace Laboratory NLR, Anthony Fokkerweg 2, 1059 CM Amsterdam, The Netherlands*
[3]*Center for Turbulence Research, Stanford University, Stanford, California 94305, USA*

(Received 30 April 2015; accepted 5 August 2015; published online 19 August 2015)

Minimum-dissipation eddy-viscosity models are a class of sub-filter models for large-eddy simulation that give the minimum eddy dissipation required to dissipate the energy of sub-filter scales. A previously derived minimum-dissipation model is the QR model. This model is based on the invariants of the resolved rate-of-strain tensor and has many desirable properties. It appropriately switches off for laminar and transitional flows, has low computational complexity, and is consistent with the exact sub-filter tensor on isotropic grids. However, the QR model proposed in the literature gives insufficient eddy dissipation. It is demonstrated that this can be corrected by increasing the model constant. The corrected QR model gives good results in simulations of decaying grid turbulence on an isotropic grid. On anisotropic grids the QR model is not consistent with the exact sub-filter tensor and requires an approximation of the filter width. It is demonstrated that the results of the QR model on anisotropic grids are primarily determined by the used filter width approximation, and that no approximation gives satisfactory results in simulations of both a temporal mixing layer and turbulent channel flow. A new minimum-dissipation model for anisotropic grids is proposed. This anisotropic minimum-dissipation (AMD) model generalizes the desirable practical and theoretical properties of the QR model to anisotropic grids and does not require an approximation of the filter width. The AMD model is successfully applied in simulations of decaying grid turbulence on an isotropic grid and in simulations of a temporal mixing layer and turbulent channel flow on anisotropic grids.  [http://dx.doi.org/10.1063/1.4928700]

## I. INTRODUCTION

Most turbulent flows cannot be computed directly from the Navier-Stokes equations because the range of scales of motion is too large. Therefore, simulations of turbulent flow often have to resort to coarse-grained models of the scales for which numerical resolution is not available. In large-eddy simulation (LES), only the large eddies in a flow are resolved and the effect of the smaller scales is modeled.[1] LES reduces the computational complexity of simulations of turbulent flow, and therefore much effort in computational fluid dynamics has been directed at the research of LES models.

The common formalization of LES reduces the range of scales in a simulation by applying a spatial filter to the Navier-Stokes equations. This gives

$$\partial_t \overline{u}_i + \partial_j \left(\overline{u}_i \overline{u}_j\right) + \partial_i \overline{p} - \partial_j \left(\nu \partial_j \overline{u}_i\right) = -\partial_j \tau_{ij}(u), \quad \partial_i \overline{u}_i = 0, \tag{1}$$

where the filter is assumed to commute with spatial derivation and $\tau_{ij}(u) = \overline{u_i u_j} - \overline{u}_i \overline{u}_j$ is the sub-filter tensor. The sub-filter tensor represents the effect of the small scales on the resolved eddies. The objective of LES modeling is to approximate the effect of sub-filter scales by closing the filtered

a)Electronic mail: w.rozema@rug.nl

 

Navier-Stokes equations with a sub-filter scale model for the tensor $\tau_{ij}(u)$ in terms of the filtered velocity field $\overline{u}$. To emphasize that a LES model is not exact,[2] the approximation of the filtered velocity is denoted $v \approx \overline{u}$, and the approximation of the filtered pressure is denoted $p \approx \overline{p}$. Thus, the objective is to formulate a sub-filter model $\tau_{ij}(v)$ so that solutions $v$ of the LES equations,

$$\partial_t v_i + \partial_j \left(v_i v_j\right) + \partial_i p - \partial_j \left(\nu \partial_j v_i\right) = -\partial_j \tau_{ij}(v), \quad \partial_i v_i = 0, \tag{2}$$

closely approximate filtered solutions $\overline{u}$ of the Navier-Stokes equations.

An important class of sub-filter models are the eddy-viscosity models. These models incorporate the effect of the unresolved eddies by locally increasing the molecular viscosity by an eddy viscosity. Eddy-viscosity models set the anisotropic part of the sub-filter model equal to

$$\tau_{ij}(v) - \frac{1}{3}\tau_{kk}(v) I_{ij} = -2\nu_e S_{ij}, \tag{3}$$

where $\nu_e$ is the eddy viscosity, and $S_{ij} = (\partial_i v_j + \partial_j v_i)/2$ is the resolved rate-of-strain tensor. The classical eddy-viscosity model is the Smagorinsky model.[3] The eddy viscosity of this model is given by $\nu_e = (C_s \delta)^2 |S|$, where $C_s$ is the Smagorinsky coefficient and $\delta$ is the filter width of the LES filter. The Smagorinsky model gives satisfactory results in simulations of decaying homogeneous isotropic turbulence.[4,5] A disadvantage of the Smagorinsky model is that it inappropriately gives eddy dissipation for laminar and transitional flows. This causes erroneous predictions of the shear stress at solid walls and delays transition to turbulence. In simulations of specific laminar or transitional flows, acceptable results can sometimes be obtained by decreasing the Smagorinsky coefficient.[6,7] However, no single value of the Smagorinsky coefficient gives satisfactory results for laminar, transitional, and turbulent flows. Therefore, the classical Smagorinsky model often fails in LES of practical flows.

The Smagorinsky model can be improved by computing the value of the Smagorinsky coefficient with the dynamic procedure.[8] The dynamic procedure determines the Smagorinsky coefficient dynamically by comparing the eddy dissipation at two filter levels. The dynamic Smagorinsky model (DSM) gives the correct level of eddy dissipation and appropriately switches off for laminar and transitional flows.[9,10] Perceived disadvantages of the dynamic Smagorinsky model are its increased computational complexity compared to the static Smagorinsky model and the need for averaging and clipping to attain numerical stability.

The Smagorinsky model gives eddy dissipation in laminar and transitional flows because its eddy viscosity does not appropriately depend on the LES solution. This disadvantage of the Smagorinsky model can also be addressed by correcting the functional dependence of the eddy viscosity on the LES solution. An example of a corrected model is the wall-adapting local eddy-viscosity (WALE) model.[11] The WALE model is designed to switch off at a desired rate near solid walls. A more fundamental take on a model that appropriately switches off for laminar flow is given by Vreman.[12] The analysis by Vreman locally characterizes a flow by the resolved velocity gradient tensor and rigorously derives the flows for which the exact sub-filter tensor gives no eddy dissipation. The eddy viscosity is then set to a positive function of the LES solution which vanishes for these flows. The resulting Vreman model is as accurate as the dynamic Smagorinsky model in simulations of a temporal mixing layer and turbulent channel flow. A perceived disadvantage of the Vreman model is that it gives eddy dissipation for back-scatter and solid body rotation. These disadvantages were the motivation for the derivation of the singular value model,[13] which is designed to switch off near solid walls and for two-dimensional flow.

This paper is about eddy-viscosity models that give the minimum eddy dissipation required to remove sub-filter scales from the LES solution. Just as the Vreman model, minimum-dissipation models can be derived from first principles. The first minimum-dissipation eddy-viscosity model is the QR model proposed by Verstappen.[14,15] The QR model has desirable practical and theoretical properties. It appropriately switches off for laminar and transitional flows, has low computational complexity, and is consistent with the exact sub-filter tensor on isotropic grids. However, simulations with the QR model have produced mixed results.[15–17]

Previous research suggests that the mixed results of the QR model are due to an incorrect model constant.[18] In this paper, it is demonstrated that the QR model produces good results on isotropic

grids if the model constant is corrected. However, it is also demonstrated that on anisotropic grids the corrected QR model is not consistent with the exact sub-filter tensor and that its results are primarily determined by a required filter width approximation. To address these disadvantages of the QR model, a new minimum-dissipation model for anisotropic grids is proposed.

## II. MINIMUM-DISSIPATION EDDY-VISCOSITY MODELS

Minimum-dissipation models give the minimum eddy dissipation required to remove the energy of sub-filter scales from the LES solution. In this paper, two minimum-dissipation models are considered. The QR model is investigated, and a new minimum-dissipation model for anisotropic grids is proposed.

### A. The QR model

In the derivation of minimum-dissipation models, sub-filter scales are defined using a box filter with domain $\Omega_\delta$ applied to the LES solution

$$\overline{v}(x) = \frac{1}{|\Omega_\delta|}\int_{\Omega_\delta} v(y)\,\mathrm{d}y, \tag{4}$$

where $x \in \Omega_\delta$. The sub-filter scales corresponding to the filter box $\Omega_\delta$ are defined as $v' = v - \overline{v}$. A minimum-dissipation model imposes that the energy of the sub-filter scales of the LES solution does not increase,

$$\partial_t \int_{\Omega_\delta} \frac{1}{2} v_i' v_i' \,\mathrm{d}x \leq 0. \tag{5}$$

Unfortunately, the evolution equation of the sub-filter energy cannot be expressed exclusively in terms of the resolved LES solution, and thus it is impossible to directly derive a practical sub-filter model from this condition. However, if the sub-filter scales are assumed to be periodic on the filter box $\Omega_\delta$, then an upper bound for the sub-filter energy can be obtained from the Poincaré inequality[15,18]

$$\int_{\Omega_\delta} \frac{1}{2} v_i' v_i' \,\mathrm{d}x \leq C_\delta \int_{\Omega_\delta} \frac{1}{2} \left(\partial_i v_j\right)\left(\partial_i v_j\right) \,\mathrm{d}x, \tag{6}$$

where the Poincaré constant $C_\delta$ is equal to the inverse of the smallest non-zero eigenvalue of the negative Laplace operator $-\partial_i\partial_i$ on the filter box $\Omega_\delta$. Payne and Weinberger have derived the Poincaré constant $C_\delta = (\delta/\pi)^2$ for a convex filter box of diameter $\delta$.[19] The Poincaré inequality suggests that the sub-filter energy of the LES solution can be confined by imposing an upper bound on the velocity gradient energy $\left(\partial_i v_j\right)\left(\partial_i v_j\right)/2$. The evolution of the velocity gradient energy density can be expressed as[15]

$$\partial_t \left( \frac{1}{2} \left(\partial_i v_j\right)\left(\partial_i v_j\right) \right) = -\left(\partial_k v_i\right)\left(\partial_k v_j\right) S_{ij} - \left(\partial_k S_{ij}\right)\partial_k\left(2\nu S_{ij}\right) - \left(\partial_k S_{ij}\right)\partial_k\left(2\nu_e S_{ij}\right) + \partial_i f_i, \tag{7}$$

where $f_i$ is a flux of velocity gradient energy. Upon spatial integration over the filter box $\Omega_\delta$, the divergence term $\partial_i f_i$ can be rewritten to a boundary integral. Boundary integrals express transport of velocity gradient energy instead of production or dissipation and are therefore ignored in the derivation of minimum-dissipation models. The production of velocity gradient energy by the convective terms can be rewritten to[15,20]

$$-\left(\partial_k v_i\right)\left(\partial_k v_j\right) S_{ij} = 4\, r(v) + \nabla\cdot(\ldots), \tag{8}$$

where

$$r(v) = -\det(S) = -\frac{1}{3}\mathrm{tr}\left(S^3\right) = -\frac{1}{3} S_{ij} S_{jk} S_{ki} \tag{9}$$

is the third invariant of the resolved rate-of-strain tensor. The dissipation rate of velocity gradient energy at the scale of the filter box $\Omega_\delta$ can be approximated by assuming that the eddy viscosity is

constant over the filter box, and application of the Poincaré inequality

$$\int_{\Omega_\delta} 2q(v)\mathrm{d}x = \int_{\Omega_\delta} S_{ij}S_{ij}\,\mathrm{d}x \leq C_\delta \int_{\Omega_\delta} \left(\partial_k S_{ij}\right)\left(\partial_k S_{ij}\right)\,\mathrm{d}x, \tag{10}$$

where

$$q(v) = \frac{1}{2}\mathrm{tr}\left(S^2\right) = \frac{1}{2}S_{ij}S_{ij} \tag{11}$$

is the second invariant of the resolved rate-of-strain tensor. Thus, an eddy-viscosity model gives sufficient eddy dissipation to cancel the production of velocity gradient energy if the inequality

$$4\int_{\Omega_\delta} r(v)\,\mathrm{d}x \leq 4\frac{\nu_e}{C_\delta}\int_{\Omega_\delta} q(v)\,\mathrm{d}x \tag{12}$$

holds. Application of the minimum eddy dissipation that satisfies this condition gives

$$\nu_e = C_\delta \frac{\max\left\{\int_{\Omega_\delta} r(v)\,\mathrm{d}x, 0\right\}}{\int_{\Omega_\delta} q(v)\,\mathrm{d}x}. \tag{13}$$

The above model is not directly applicable in a practical LES, because the exact integrals of invariants are not available. Previous applications of the QR model have used the mid-point rule to approximate the integrals and a numerical approximation of the Poincaré constant. This gives the point-wise model

$$\nu_e = C\delta^2 \frac{\max\left\{r(v), 0\right\}}{q(v)}, \tag{14}$$

where $C$ is a model constant and $\delta$ is the LES filter width. This is the QR model used in this paper.

The QR model has desirable practical and theoretical properties. It can be shown that the third invariant of the rate-of-strain tensor vanishes in flows that are laminar according to the analysis by Vreman.[12] Thus, the QR model gives zero eddy dissipation for the same flows as the exact sub-filter tensor. In contrast to the Vreman model, the QR model also switches off for back-scatter and two-dimensional flow.[13,15] Also, the computational complexity of the QR model is low. Compared to the classical Smagorinsky model, the QR model needs only additional computation of the third invariant of a tensor which is already available. Finally, the production term in Eq. (7) is proportional to the dissipation of the leading-order term of a Taylor expansion of the exact sub-filter tensor on isotropic grids.[7,12] This dissipation is proportional to the third invariant $r(v)$ by Eq. (8), and thus on isotropic grids, the QR model is consistent with the eddy dissipation of the exact sub-filter tensor. This consistency is a desirable theoretical property, but unfortunately does not hold on anisotropic grids.

### B. The model constant and filter width of the QR model

Application of the QR model in a practical LES requires setting of the model constant $C$. In the literature, the model constant has effectively been set to $C = 1/8$ for second-order accurate methods.[15] In a previous publication, we have demonstrated that this constant gives insufficient eddy dissipation.[18]

The appropriate constant of a sub-filter model depends on the numerical method and on the nature of the turbulence at the cutoff of the LES filter.[21] Thus, the constant of a sub-filter model cannot be determined uniquely, but there is a range of appropriate model constants.[13] If the QR model is discretized to the same order of accuracy as the numerical method, then satisfactory results are obtained in a simulation of decaying grid turbulence if the constant of the QR model is set to $C = 1/3$ for a central second-order accurate method and to $C = 0.236$ for a central fourth-order accurate method. These corrected model constants are considerably larger than the model constants proposed in the literature, which raises doubts about results of previous simulations with the QR model.[15–17]

On isotropic grids, the LES filter width $\delta$ of the QR model is set equal to the grid spacing

$$\delta = \Delta x_1 = \Delta x_2 = \Delta x_3, \tag{15}$$

where $\Delta x_1$, $\Delta x_2$, and $\Delta x_3$ denote the grid spacing in the three spatial directions. On anisotropic grids, the QR model requires approximation of the filter width $\delta$. In the literature, the filter width has been set according to a numerical counterpart of the Poincaré constant[15]

$$\frac{3}{\delta^2} = \frac{1}{\Delta x_1^2} + \frac{1}{\Delta x_2^2} + \frac{1}{\Delta x_3^2}. \tag{16}$$

For grid cells with a large aspect ratio, this filter width approximation is dominated by the grid spacing in the finest grid direction. A more conventional approximation of the filter width on anisotropic grids is given by the geometric mean[6]

$$\delta = (\Delta x_1 \Delta x_2 \Delta x_3)^{1/3}. \tag{17}$$

On anisotropic grids the above approximations give different filter widths. In this paper, it will be demonstrated that on anisotropic grids the results of the QR model are primarily determined by the used approximation of the filter width, and that no approximation gives satisfactory results in simulations of both a temporal mixing layer and turbulent channel flow.

Sensitivity of the QR model to the used filter width approximation on anisotropic grids raises doubts about the practical applicability of the QR model. Also, whereas the QR model is consistent with the exact sub-filter tensor on isotropic grids, this desirable property does not hold on anisotropic grids. This motivates the derivation of a minimum-dissipation model which does not require an approximation of the filter width and is consistent with the exact sub-filter tensor on both isotropic and anisotropic grids.

### C. A new minimum-dissipation model for anisotropic grids

The derivation of the QR model applies the box filter to the LES solution and confines the energy of sub-filter scales by application of the Poincaré inequality. This gives a model constant $C_\delta$ which depends on the size of the filter box. On anisotropic grids this dependence has to be approximated, which introduces sensitivity to the used filter width approximation.

The dependence of the model constant on the size of the filter box can be sidestepped by using a modified Poincaré inequality. For simplicity, it is assumed that the filter box $\Omega_\delta$ is rectangular with dimensions $\delta x_1$, $\delta x_2$, and $\delta x_3$. The energy of the sub-filter scales can then be confined using a modified Poincaré inequality

$$\int_{\Omega_\delta} \frac{1}{2} v_i' v_i' \, \mathrm{d}x \leq C \int_{\Omega_\delta} \frac{1}{2} \left(\delta x_i \partial_i v_j\right) \left(\delta x_i \partial_i v_j\right) \, \mathrm{d}x, \tag{18}$$

where $(\delta x_i \partial_i)$ is the scaled gradient operator, $\left(\delta x_i \partial_i v_j\right)\left(\delta x_i \partial_i v_j\right)/2$ is the scaled velocity gradient energy, and $C$ is a modified Poincaré constant. The modified Poincaré constant $C$ is equal to the inverse of the smallest non-zero eigenvalue of the negative scaled Laplace operator $-(\delta x_i \partial_i)(\delta x_i \partial_i)$ integrated over the filter box $\Omega_\delta$, which is independent of the size of the filter box. Thus, whereas the Poincaré inequality in Eq. (6) incorporates the dependence on the size of the filter box in the Poincaré constant $C_\delta$, the modified Poincaré inequality incorporates the dependence on the size of the filter box by scaling the velocity gradient.

The modified Poincaré inequality demonstrates that the sub-filter energy can be confined by imposing a bound on the scaled velocity gradient energy. If the eddy viscosity and the filter widths are assumed to be constant on the filter box $\Omega_\delta$, then the evolution equation for the scaled velocity gradient energy density on the filter box can be expressed as

$$\begin{aligned} \partial_t \left( \frac{1}{2} \left(\delta x_i \partial_i v_j\right) \left(\delta x_i \partial_i v_j\right) \right) = &- \left(\delta x_k \partial_k v_i\right) \left(\delta x_k \partial_k v_j\right) S_{ij} \\ &- \left(\nu + \nu_e\right) \delta x_k \partial_k \left(\partial_i v_j\right) \delta x_k \partial_k \left(\partial_i v_j\right) + \partial_i f_i. \end{aligned} \tag{19}$$

In contrast to the derivation of the QR model, the production and dissipation of scaled velocity gradient energy are not expressed in terms of invariants of the rate-of-strain tensor. Instead, the production and dissipation are expressed in terms of the velocity gradient.

The dissipation at the scale of a filter box can be approximated by application of the modified Poincaré inequality

$$\int_{\Omega_\delta} \left(\partial_i v_j\right)\left(\partial_i v_j\right) \,\mathrm{d}x \leq C \int_{\Omega_\delta} \delta x_k \partial_k \left(\partial_i v_j\right) \delta x_k \partial_k \left(\partial_i v_j\right) \mathrm{d}x. \tag{20}$$

Thus, the eddy-viscosity model gives sufficient eddy dissipation to cancel the production of scaled velocity gradient energy if the inequality

$$\int_{\Omega_\delta} -\left(\delta x_k \partial_k v_i\right)\left(\delta x_k \partial_k v_j\right) S_{ij} \,\mathrm{d}x \leq \frac{\nu_e}{C} \int_{\Omega_\delta} \left(\partial_i v_j\right)\left(\partial_i v_j\right) \,\mathrm{d}x \tag{21}$$

holds. Taking the minimum eddy dissipation that satisfies this condition gives

$$\nu_e = C \frac{\max\left\{\int_{\Omega_\delta} -\left(\delta x_k \partial_k v_i\right)\left(\delta x_k \partial_k v_j\right) S_{ij} \,\mathrm{d}x, 0\right\}}{\int_{\Omega_\delta} \left(\partial_l v_m\right)\left(\partial_l v_m\right) \,\mathrm{d}x}. \tag{22}$$

In practical applications of this model, the integrals over the filter box are approximated by the mid-point rule for integration

$$\nu_e = C \frac{\max\left\{-\left(\delta x_k \partial_k v_i\right)\left(\delta x_k \partial_k v_j\right) S_{ij}, 0\right\}}{\left(\partial_l v_m\right)\left(\partial_l v_m\right)}. \tag{23}$$

This is the eddy viscosity of the anisotropic minimum-dissipation (AMD) model. The computational complexity of the AMD model is comparable to the computational complexity of the QR model. In practical applications of the AMD model, the size of the filter box is set equal to the size of a grid cell $\delta x_i = \Delta x_i$. If the model is discretized to the same order of accuracy as the Navier-Stokes equations, then simulations of decaying grid turbulence give satisfactory results if the model constant is set to $C = 0.300$ for a central second-order accurate method and to $C = 0.212$ for a central fourth-order accurate method.

The AMD model is consistent with the exact sub-filter tensor on anisotropic grids. Taylor expansion of the sub-filter tensor gives[22]

$$\tau_{ij}(u) = \overline{u_i u_j} - \overline{u}_i \overline{u}_j = \frac{1}{12} \left(\delta x_k \partial_k v_i\right)\left(\delta x_k \partial_k v_j\right) + O(\delta x_i^4). \tag{24}$$

Thus, the eddy dissipation of the exact sub-filter tensor is

$$-\tau_{ij} S_{ij} = -\frac{1}{12} \left(\delta x_k \partial_k v_i\right)\left(\delta x_k \partial_k v_j\right) S_{ij} + O(\delta x_i^4). \tag{25}$$

The leading-order term of this expansion is proportional to the term in the numerator of the eddy viscosity of the AMD model. This demonstrates consistency of the AMD model with the exact eddy dissipation. The leading-order term of the Taylor expansion of the exact sub-filter tensor is also known as the gradient sub-filter model.[7] Thus, the AMD model gives eddy dissipation if the gradient model gives eddy dissipation. Consistency with the gradient model is a desirable property. According to *a priori* tests, the gradient model has good correlation with the exact sub-filter tensor.[22] Also, if the analysis by Vreman is restricted to separable filters, then the gradient model gives zero eddy dissipation for the same flows as the exact sub-filter tensor.[12] This confirms that the AMD model switches off for flows with vanishing exact eddy dissipation. In contrast to the Vreman model, the AMD model also switches off for back-scatter and for two-dimensional flow on isotropic grids.

In conclusion, the proposed minimum-dissipation model for anisotropic grids has desirable practical and theoretical properties. The AMD model appropriately switches off if no sub-filter energy is being created and has low computational complexity. In contrast to the QR model, on anisotropic grids the AMD model is consistent with the exact sub-filter tensor and does not require an approximation of the filter width.

## III. RESULTS

To validate the proposed minimum-dissipation models, simulations are performed of decaying grid turbulence, a temporal mixing layer, and turbulent channel flow. The simulations have been performed with two kinetic energy conserving methods: a central discretization of the compressible Navier-Stokes equations on collocated computational grids[23,24] and a central symmetry-preserving discretization of the incompressible Navier-Stokes equations on staggered grids.[25] In both simulation methods, the eddy viscosity of the sub-filter model is computed at cell centers with the same order of accuracy as the Navier-Stokes equations.

### A. Decaying grid turbulence

To assess the applicability of the minimum-dissipation models to decaying homogeneous isotropic turbulence, simulations of the decaying grid turbulence experiment by Comte-Bellot and Corrsin are performed.[26] In these experiments, turbulence is generated by a grid with mesh size $M = 5.08$ cm in a flow of mean velocity $U_0 = 1000$ cm/s. Energy spectra of the decaying turbulence are recorded at three stations $42M$, $98M$, and $171M$ downstream of the grid. The simulations are simplified by considering the flow inside a cube of length $11M$ which moves along with the mean flow and passes the grid at $t = 0$ s. Thus, the turbulence in the cube is expected to match with the measured energy spectra at $t = 42M/U_0$, $t = 98M/U_0$, and $t = 171M/U_0$. All the quantities are non-dimensionalized by the length of the cube $L_{\text{ref}} = 11M = 55.88$ cm and a reference velocity $u_{\text{ref}} = 27.19$ cm/s, which satisfies $u_{\text{ref}}^2 = 3\overline{u_1^2}/2$ at the first measurement station.

The simulations are performed with the collocated method for compressible flow. To assess the influence of the numerical discretization, the method is used at both second-order and fourth-order accuracy. Simulations are performed with the DSM,[27] the QR model in Eq. (14), and the AMD model in Eq. (23). The DSM is implemented with a box filter as test filter and with averaging of the minimization error in the homogeneous directions. The QR model is used with the model constant proposed in the literature $C = 1/8$ and with the corrected model constant $C = 1/3$. The computational grid is isotropic with 64 cells in each direction. The Reynolds number based on the size of the computational domain is $\text{Re} = 10\,129$, and the dimensionless time step size is set to $\Delta t' = 1.59 \times 10^{-3}$. The initial condition is generated by fitting a velocity field with randomized phases to the spectrum measured at the first station. The random phases are adjusted by performing a preliminary simulation from $t = 0$ s to $t = 42M/U_0$ and fitting the adjusted velocity field to the spectrum measured at the first station.[28] The resulting field is used as the initial condition for the simulations.

Figure 1 shows the energy decay and energy spectra obtained with the second-order accurate simulation method with the DSM and the minimum-dissipation models. The data points in the energy decay plot have been obtained by fitting the measured energy spectra to the computational grid and computing the total kinetic energy. Results obtained with the QR model are sensitive to the model constant. The energy dissipation obtained with the model constant $C = 1/8$ is considerably smaller than the energy dissipation observed in experiments. However, the energy dissipation obtained with the corrected model constant $C = 1/3$ accurately agrees with the measured energy dissipation. The energy decay predicted by the AMD model also closely agrees with the experiment. The energy decay obtained with the DSM agrees with the box-filtered experiment instead of the unfiltered experiment. This is consistent with the implementation of the DSM, which assumes that the LES filter is a box filter.

The computed energy spectra demonstrate that the QR model gives an erroneous accumulation of resolved kinetic energy at scales near the grid cutoff for the model constant proposed in the literature $C = 1/8$. This indicates that the QR model does not give sufficient eddy dissipation to eliminate sub-filter scales from the LES solution for this constant. For the corrected model constant $C = 1/3$, the QR model captures the turbulent energy cascade appropriately. Energy spectra obtained with the AMD model are as accurate as energy spectra obtained with the corrected QR model. The energy spectra obtained with minimum-dissipation models differ from energy spectra obtained with the DSM at wave numbers near the grid cutoff. The minimum-dissipation models give the minimum

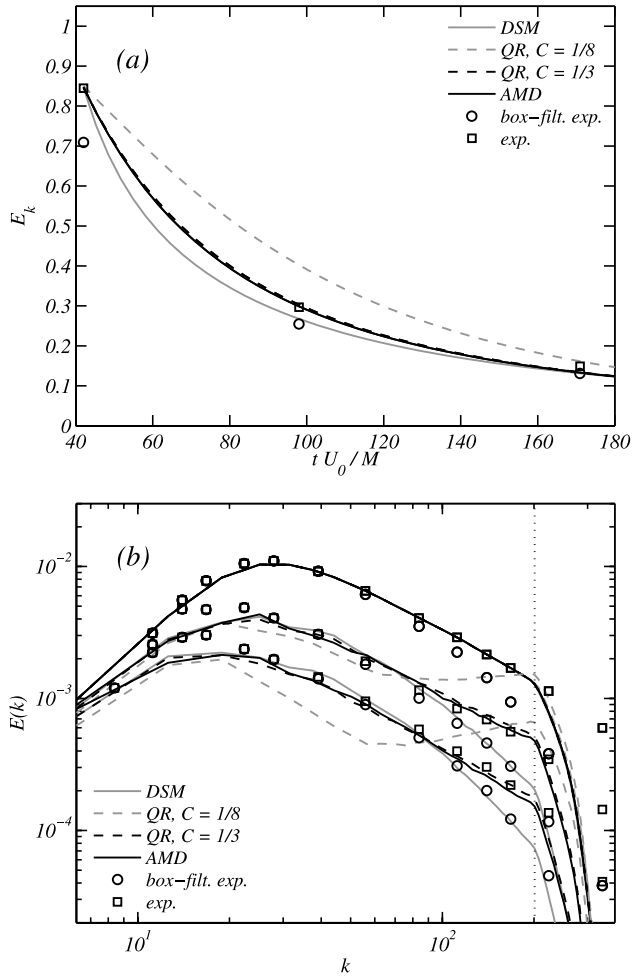


FIG. 1. The kinetic energy decay (a) and the energy spectra at the three measurement stations (b) obtained with the second-order accurate simulation method with the DSM, the QR model with the constant $C = 1/8$, the QR model with the corrected constant $C = 1/3$, and the AMD model.

eddy dissipation required to remove the sub-filter scales from the LES solution, and the energy spectra agree with the experiment at all the resolved wave numbers. However, the DSM agrees with the box-filtered experiment, and the obtained energy spectra fall off at wave numbers near the grid cutoff.

Figure 2 shows the energy decay and energy spectra obtained with the fourth-order accurate simulation method with the DSM, the corrected QR model, and the AMD model. The energy decay obtained with the corrected QR model and the AMD model closely agrees with the experiment. Also, the computed energy spectra demonstrate that both the minimum-dissipation models appropriately capture the turbulent energy cascade. Thus, the proposed minimum-dissipation models can successfully capture decaying grid turbulence in simulation methods of both second-order and fourth-order accuracy.

### B. Temporal mixing layer

To assess the applicability of minimum-dissipation models to transitional flow on anisotropic grids, simulations of a temporal mixing layer are performed. A temporal mixing layer consists of two streams with opposite flow velocities. A Kelvin-Helmholtz instability originates at the interface of the two streams and eventually causes transition to turbulence of the mixing layer. The temporal mixing layer is expected to be self-similar in the turbulent regime.[29,30]

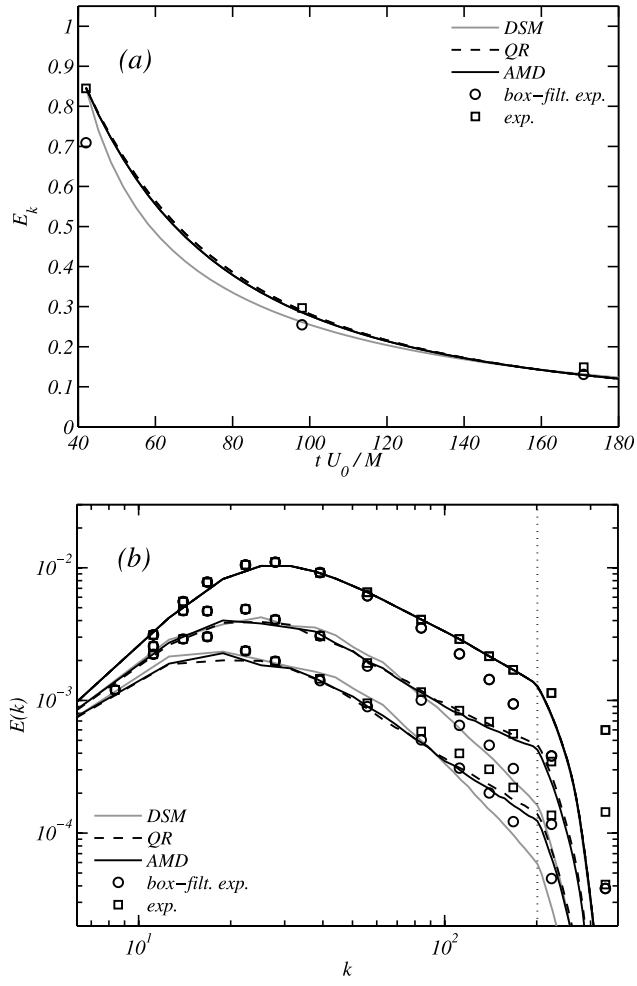


FIG. 2. The kinetic energy decay (a) and the energy spectra at the three measurement stations (b) obtained with the fourth-order accurate simulation method with the DSM, the corrected QR model, and the AMD model.

The temporal mixing layer studied in this paper is similar to the weakly compressible mixing layer at a high Reynolds number studied by Vreman.[12] The coordinate $x$ is aligned with the stream-wise direction, the coordinate $y$ with the direction normal to the mixing layer, and the coordinate $z$ with the span-wise direction. All the quantities are non-dimensionalized by half the initial vorticity thickness of the mixing layer, the far-field stream-wise velocity, and the free-stream temperature and pressure. The initial dimensionless velocity field is given by a hyperbolic tangent

$$u = \tanh(y), \quad v = 0, \quad w = 0, \tag{26}$$

and random perturbations of a small magnitude are added near the center plane $y = 0$ to trigger transition to turbulence. The initial non-dimensionalized temperature profile is set to

$$T = 1 + \frac{1}{2}(\gamma - 1)M^2(1 - u)(1 + u), \tag{27}$$

where $\gamma$ is the heat capacity ratio and $M$ is the free-stream Mach number. The initial pressure is set equal to the free-stream pressure $p = 1$. The Reynolds number based on half the initial vorticity thickness is 100 000, and the free-stream Mach number is $M = 0.25$. The computational domain spans 90 times half the initial vorticity thickness in each direction. The simulations are performed on anisotropic rectangular grids with constant grid spacing in each direction. The grids have 90 cells in the stream-wise and span-wise directions, and 180, 360, or 720 grid cells in the direction normal to the mixing layer. Thus, the cells of the computational grids have aspect ratios $\Delta x/\Delta y = \Delta z/\Delta y$

of 2, 4, and 8, respectively. The boundary conditions in the stream-wise and span-wise directions are periodic, and free-slip boundary conditions are imposed at the boundaries in the direction normal to the mixing layer.

The simulations are performed with the fourth-order accurate collocated method for compressible flow. Simulations are performed with the DSM, the Vreman model, the corrected QR model, and the AMD model. On anisotropic grids, the QR model requires an approximation of the filter width. Simulations are performed with the approximation proposed in the literature in Eq. (16) and with the conventional approximation in Eq. (17). The results of the simulations are presented as plots of the growth rate of the momentum thickness $\theta$ of the mixing layer, the variance of the stream-wise velocity $\langle u'u' \rangle$, the dissipation rate of total kinetic energy, and stream-wise energy spectra at the center plane of the mixing layer.

First, the results obtained on the grid with an aspect ratio of 4 are presented. Figure 3 shows the growth rate of the mixing layer and the variance of the stream-wise velocity obtained with the AMD model in the turbulent regime. The DSM and the Vreman model are known to appropriately switch off for transitional flow.[7,12] Transition of the mixing layer occurs at approximately the same time for the DSM and the Vreman model. For both models, the growth rate of the mixing layer is approximately constant from $t = 50$ to $t = 140$, which indicates self-similarity of the mixing layer in the turbulent regime.

The minimum-dissipation models predict transition to turbulence at approximately the same time as the DSM and the Vreman model. This suggests that the minimum-dissipation models appropriately switch off for transitional flow. The behavior of the QR model in the turbulent regime is primarily determined by the approximation of the filter width. For the conventional filter width approximation in Eq. (17), the growth rate of the mixing layer is approximately equal to the growth rate predicted by the DSM, but for the filter width approximation in Eq. (16), the growth rate is considerably smaller. The AMD model does not require an approximation of the filter width on anisotropic grids, and predicts a growth rate which closely agrees with the growth rate obtained with the DSM and the Vreman model. Plots of the variance of the stream-wise velocity obtained with the AMD model at different times in the turbulent regime approximately collapse. This indicates that the AMD model appropriately captures the self-similar character of the mixing layer in the turbulent regime.

Figure 4 shows the dissipation rate of total kinetic energy and the stream-wise energy spectra at $t = 140$. The dissipation rate obtained with the DSM, the Vreman model, and the minimum-dissipation models is practically zero up to $t = 25$, which confirms that the models appropriately switch off for transitional flow. The DSM, the Vreman model, the QR model with the filter width approximation in Eq. (17), and the AMD model predict approximately equal dissipation rates in the turbulent regime. However, the QR model with the filter width approximation in Eq. (16) predicts a dissipation rate which is larger up to approximately $t = 100$ and smaller afterwards. The

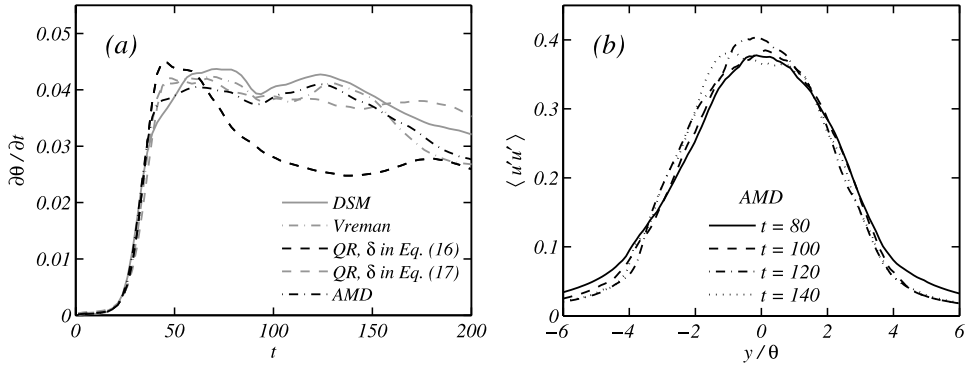


FIG. 3. The growth rate of the momentum thickness obtained in simulations of the temporal mixing layer on the grid with an aspect ratio of 4 with the DSM, the Vreman model, the QR model with two approximations of the filter width, and the AMD model (a), and the variance of the stream-wise velocity as a function of the normalized normal coordinate obtained with the AMD model at different times (b).

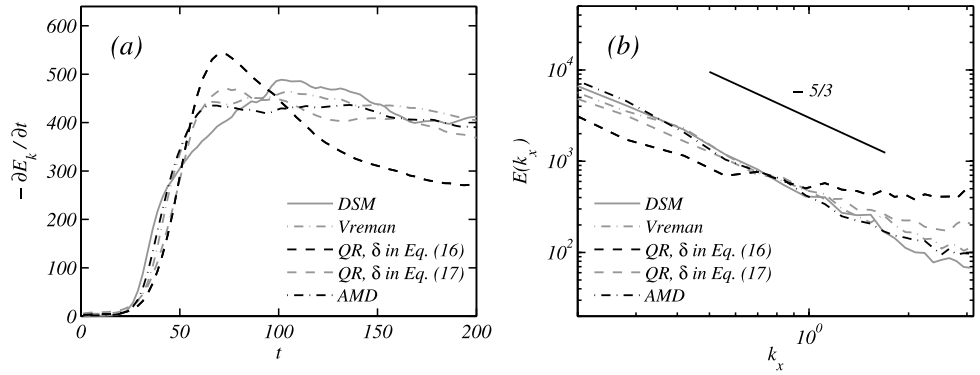


FIG. 4. The decay rate of the total energy (a) and the stream-wise energy spectra at the center plane of the mixing layer at $t = 140$ (b) obtained in simulations of the temporal mixing layer on the grid with an aspect ratio of 4 with the DSM, the Vreman model, the QR model with two approximations of the filter width, and the AMD model.

energy spectra show a marked quantitative difference of results obtained with the QR model for the two filter width approximations. The DSM, the Vreman model, and the QR model with the filter width approximation in Eq. (17), and the AMD model give energy spectra with the desirable $E(k_x) \sim k_x^{-5/3}$ decay rate. However, the QR model with the filter width approximation proposed in the literature in Eq. (16) gives accumulation of energy at scales near the grid cutoff. This indicates that the QR model does not give sufficient eddy dissipation on anisotropic grids for this filter width approximation.

Figure 5 shows results of simulation on the grids with aspect ratios of 2 and 8. The results confirm that on grids with considerable anisotropy, the behavior of the QR model is primarily

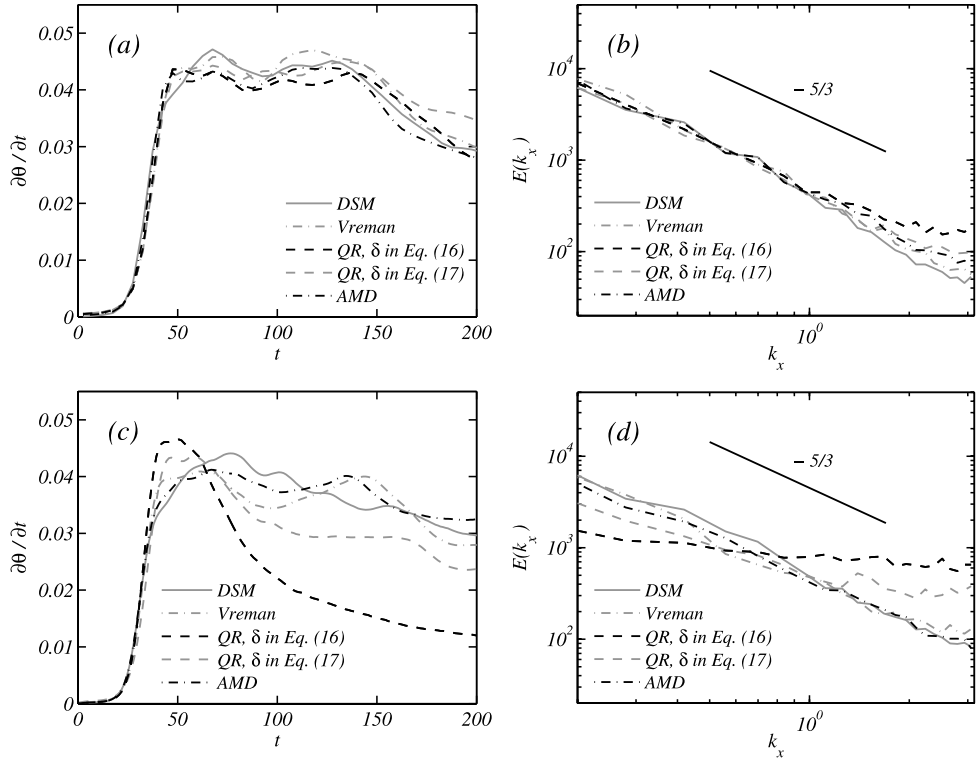


FIG. 5. The growth rate of the momentum thickness and the stream-wise energy spectra at the center plane of the mixing layer at $t = 140$ obtained in simulations of the temporal mixing layer on the grids with aspect ratios of 2 (a) and (b), and 8 (c) and (d) with the DSM, the Vreman model, the QR model with two approximations of the filter width, and the AMD model.

determined by the filter width approximation. On the grid with the smaller aspect ratio of 2, results obtained with both the filter width approximations closely agree with results obtained with the DSM and the Vreman model. However, on the grid with the larger aspect ratio of 8, the QR model behaves differently for the two considered filter width approximations. The filter width approximation in Eq. (16) gives a considerably smaller growth rate in the turbulent regime than the DSM and the Vreman model. The conventional filter width approximation in Eq. (17) gives a larger growth rate but does not attain the growth rate predicted by the DSM and the Vreman model. On the grid with the aspect ratio of 8, the QR model gives accumulation of kinetic energy near the grid cutoff for both the filter width approximations. This indicates that the QR model gives insufficient eddy dissipation for both the filter width approximations.

The AMD model does not require an approximation of the filter width, and its results closely agree with results obtained with the DSM and the Vreman model at both the aspect ratios 2 and 8. The AMD model appropriately switches off for transitional flow and correctly captures the constant growth rate of the mixing layer in the turbulent regime. Also, the AMD model gives energy spectra with the desirable decay rate at both the aspect ratios.

### C. Turbulent channel flow

To assess the applicability of the proposed minimum-dissipation models to wall-bounded flow, simulations of turbulent channel flow at a friction Reynolds number of $\mathrm{Re}_\tau \approx 590$ are performed.[31] The coordinate $x$ is aligned with the stream-wise direction of the channel, the coordinate $y$ with the wall-normal direction, and the coordinate $z$ with the span-wise direction. The size of the channel is $2\pi H \times 2H \times \pi H$, where $H$ is the channel half-height. The initial condition is set to a Poiseuille flow with a bulk velocity $u_b$. Divergence-free perturbations of a small magnitude are superimposed to the initial condition to trigger transition to turbulence. The channel flow is driven by a uniform mass flux which fixes the bulk Reynolds number $\mathrm{Re}_b = u_b H/\nu$ at 10 975. After the channel flow has transitioned to turbulence, flow statistics are recorded. Important outputs of the simulations are the wall shear stress $\tau_w$, the corresponding friction velocity $u_\tau = \sqrt{\tau_w/\rho}$, and friction Reynolds number $\mathrm{Re}_\tau = u_\tau H/\nu$.

Large-eddy simulations are performed with the second-order accurate method for incompressible flow on staggered grids. The simulations are performed on a coarse grid with 64 cells in each direction. The grid spacing is uniform in the stream-wise and span-wise directions. In the wall-normal direction, the grid stretches towards the wall according to a hyperbolic sine distribution.[25] The height of the first grid cell at the wall is $\Delta y^+ = 3.9$ in viscous length scales. Simulations are performed without sub-filter model, with the DSM, with the QR model, and with the AMD model. For the QR model, the filter width is set according to the approximation in Eq. (16) and according to the approximation in Eq. (17). The results of the large-eddy simulations are compared with results of the direct numerical simulation (DNS) by Moser *et al.*[31]

Table I lists the friction Reynolds numbers computed in the simulations. Figure 6 shows the mean stream-wise flow velocity and the turbulent fluctuations normalized by the computed friction velocity. A simulation without model predicts a friction Reynolds number which significantly exceeds the actual friction Reynolds number. The DSM and the AMD model give satisfactory predictions of both the friction Reynolds number and the mean flow velocity. Just as in simulations of the temporal mixing layer, results obtained with the QR model are primarily determined by the used filter width approximation. Results obtained with the filter width approximation in Eq. (16)

TABLE I. The friction Reynolds numbers obtained in large-eddy simulations of channel flow at a bulk Reynolds number $\mathrm{Re}_b = 10\,975$ and the relative error with respect to the friction Reynolds number obtained in a DNS.

| No model | DSM | QR, $\delta$ in Eq. (16) | QR, $\delta$ in Eq. (17) | AMD | DNS |
|---|---|---|---|---|---|
| 618.6 | 570.6 | 587.8 | 509.5 | 578.8 | 587.2 |
| 5.3% | −2.8% | 0.1% | −13.2% | −1.4% | |

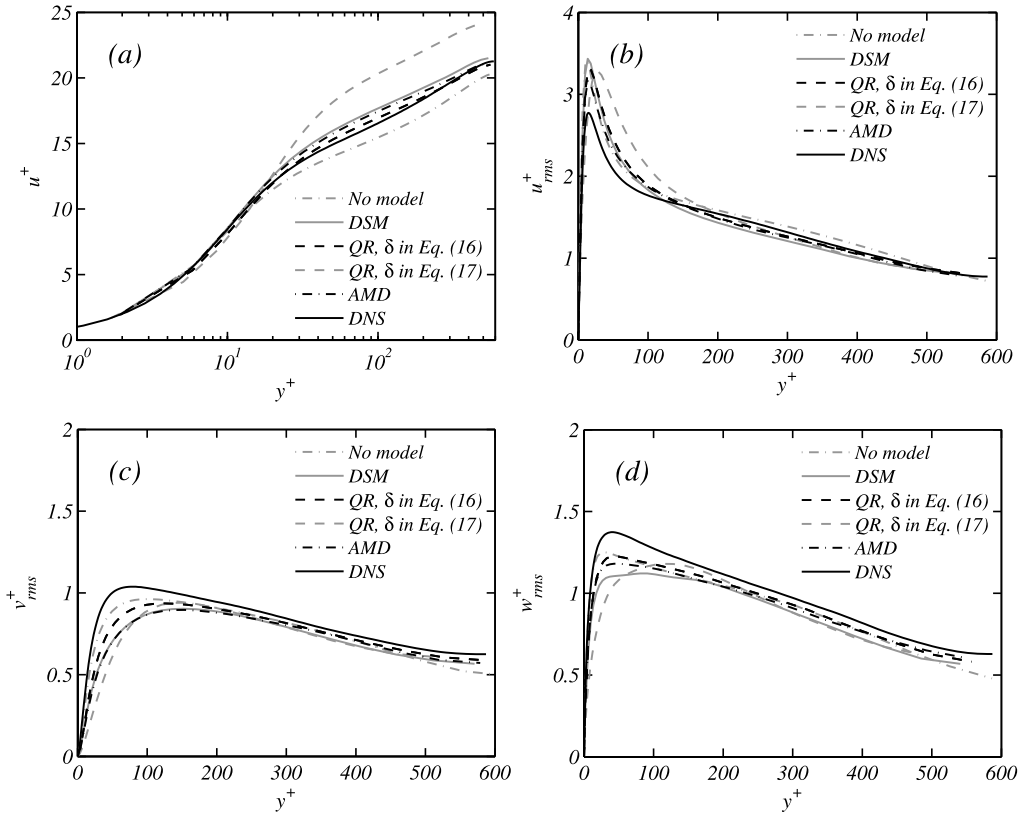


FIG. 6. The normalized mean flow velocity (a) and the turbulent fluctuations in the stream-wise (b), span-wise (c), and wall-normal (d) directions obtained in simulations of channel flow at a bulk Reynolds number $\mathrm{Re}_b = 10\,975$.

closely agree with the DNS, but the filter width approximation in Eq. (17) is too dissipative. This is in contrast with the simulations of the temporal mixing layer, where the filter width approximation in Eq. (17) gives more accurate results than the filter width approximation in Eq. (16).

It is well-known that the accuracy of channel flow simulations with eddy-viscosity models is mainly determined by the behavior of the sub-filter model near the wall.[32] The near-wall behavior of the two considered filter width approximations is different. Possibly, the results of channel flow simulations with the QR model actually assess the ability of the used filter width approximation to act as a wall damping function and not whether the QR model appropriately depends on the LES solution.

## IV. CONCLUSION

The previously proposed QR sub-filter model was investigated. The QR model gives the minimum eddy dissipation required to remove sub-filter scales from the LES solution and appropriately switches off for laminar and transitional flows. The model has low computational complexity and is consistent with the exact sub-filter tensor on isotropic grids. The QR model proposed in the literature gives insufficient eddy dissipation. It was demonstrated that this can be corrected by increasing the model constant. The corrected QR model gives satisfactory results in simulations of decaying grid turbulence on an isotropic grid. On anisotropic grids, the QR model is not consistent with the exact sub-filter tensor and requires an approximation of the filter width. Results obtained with the QR model on anisotropic grids are primarily determined by the used filter width approximation, and no approximation gives acceptable results in simulations of both a temporal mixing layer and turbulent channel flow. To address this flaw of the QR model, a new minimum-dissipation model for anisotropic grids was proposed. The AMD model appropriately switches off in laminar and

transitional flows and has low computational complexity. The model is consistent with the exact sub-filter tensor on both isotropic and anisotropic grids and does not require an approximation of the filter width. The AMD model gives accurate results in simulations of decaying grid turbulence on an isotropic grid and in simulations of a temporal mixing layer and turbulent channel flow on anisotropic grids. Thus, unlike the QR model, the AMD model is suitable for practical LES on anisotropic grids.

## ACKNOWLEDGMENTS

A part of this research was conducted at the Stanford CTR summer program 2014. W.R. and R.V. are grateful for the opportunity to participate in this program, the received financial support, and the interactions with the CTR staff and the participants of the summer program. W.R. receives financial support from the Ubbo Emmius Fund of the University of Groningen and kindly acknowledges support from the National Aerospace Laboratory NLR. W.R. and R.V. acknowledge sponsoring by the Netherlands Organization for Scientific Research (NWO) for the use of supercomputing facilities. H.J.B. receives financial support from the Stanford Graduate Fellowship.

[1] C. Meneveau and P. Sagaut, *Large Eddy Simulation for Incompressible Flows: An Introduction* (Springer Science & Business Media, 2006).
[2] J.-L. Guermond, J. T. Oden, and S. Prudhomme, "Mathematical perspectives on large eddy simulation models for turbulent flows," J. Math. Fluid Mech. **6**, 194–248 (2004).
[3] J. Smagorinsky, "General circulation experiments with the primitive equations. I. The basic experiment," Mon. Weather Rev. **91**, 99–164 (1963).
[4] D. K. Lilly, "On the application of the eddy viscosity concept in the inertial sub-range of turbulence," Technical Report No. 123, National Center for Atmospheric Research, 1966.
[5] N. N. Mansour, P. Moin, W. C. Reynolds, and J. H. Ferziger, "Improved methods for large eddy simulations of turbulence," in *Turbulent Shear Flows 1* (Springer-Verlag, 1979), pp. 386–401.
[6] J. W. Deardorff, "A numerical study of three-dimensional turbulent channel flow at large Reynolds numbers," J. Fluid Mech. **41**, 453–480 (1970).
[7] A. W. Vreman, "Direct and large-eddy simulation of the compressible turbulent mixing layer," Ph.D. thesis, Universiteit Twente, 1995.
[8] M. Germano, U. Piomelli, P. Moin, and W. H. Cabot, "A dynamic subgrid-scale eddy viscosity model," Phys. Fluids A **3**, 1760–1765 (1991).
[9] U. Piomelli, "High Reynolds number calculations using the dynamic subgrid-scale stress model," Phys. Fluids A **5**, 1484–1490 (1973).
[10] C. Meneveau and J. Katz, "Scale-invariance and turbulence models for large-eddy simulation," Annu. Rev. Fluid Mech. **32**, 1–32 (2000).
[11] F. Nicoud and F. Ducros, "Subgrid-scale stress modelling based on the square of the velocity gradient," Flow, Turbul. Combust. **62**, 183–200 (1999).
[12] A. W. Vreman, "An eddy-viscosity subgrid-scale model for turbulent shear flow: Algebraic theory and applications," Phys. Fluids **16**, 3670–3681 (2004).
[13] F. Nicoud, H. B. Toda, O. Cabrit, S. Bose, and J. Lee, "Using singular values to build a subgrid-scale model for large eddy simulations," Phys. Fluids **23**, 085106 (2011).
[14] R. W. C. P. Verstappen, S. T. Bose, J. Lee, H. Choi, and P. Moin, "A dynamic eddy-viscosity model based on the invariants of the rate-of-strain," in *Proceedings of the Summer Program* (Center for Turbulence Research, Stanford University, 2010), pp. 183–192.
[15] R. Verstappen, "When does eddy viscosity damp subfilter scales sufficiently?," J. Sci. Comput. **49**, 94–110 (2011).
[16] D. E. Aljure, O. Lehmkuhl, I. Rodriguez, and A. Oliva, "Flow and turbulent structures around simplified car models," Comput. Fluids **96**, 122–135 (2014).
[17] A. E. P. Veldman, R. Luppes, H. J. L. van der Heiden, P. van der Plas, B. Duz, and R. H. M. Huijsmans, "Turbulence modeling, local grid refinement and absorbing boundary conditions for free-surface flow simulations in offshore applications," in *Proceedings of the 33rd International Conference on Ocean, Offshore and Arctic Engineering, San Fransisco, USA* (ASME, 2014), OMAE2014-24427.
[18] R. W. C. P. Verstappen, W. Rozema, and H. J. Bae, "Numerical scale separation in large-eddy simulation," in *Proceedings of the Summer Program* (Center for Turbulence Research, Stanford University, 2014), pp. 417–426.
[19] L. Payne and H. F. Weinberger, "An optimal Poincaré inequality for convex domains," Arch. Ration. Mech. Anal. **5**, 286–292 (1960).
[20] D. Chae, "On the spectral dynamics of the deformation tensor and new *a priori* estimates for the 3D Euler equations," Commun. Math. Phys. **263**, 789–801 (2006).
[21] C. Meneveau and T. S. Lund, "The dynamic Smagorinsky model and scale-dependent coefficients in the viscous range of turbulence," Phys. Fluids **9**, 3932–3934 (1997).
[22] R. A. Clark, J. H. Ferziger, and W. C. Reynolds, "Evaluation of subgrid-scale models using an accurately simulated turbulent flow," J. Fluid Mech. **91**, 1–16 (1979).

[23] J. C. Kok, "A high-order low-dispersion symmetry-preserving finite-volume method for compressible flow on curvilinear grids," J. Comput. Phys. **228**, 6811–6832 (2009).
[24] W. Rozema, J. C. Kok, R. W. C. P. Verstappen, and A. E. P. Veldman, "A symmetry-preserving discretisation and regularisation model for compressible flow with application to turbulent channel flow," J. Turbul. **15**, 386–410 (2014).
[25] R. W. C. P. Verstappen and A. E. P. Veldman, "Symmetry-preserving discretization of turbulent flow," J. Comput. Phys. **187**, 343–368 (2003).
[26] G. Comte-Bellot and S. Corrsin, "Simple Eulerian time correlation of full- and narrow-band velocity signals in grid-generated, 'isotropic' turbulence," J. Fluid Mech. **48**, 273–337 (1971).
[27] D. K. Lilly, "A proposed modification of the Germano subgrid-scale closure method," Phys. Fluids A **4**, 633–635 (1992).
[28] H. S. Kang, S. Chester, and C. Meneveau, "Decaying turbulence in an active-grid-generated flow and comparisons with large-eddy simulation," J. Fluid Mech. **480**, 129–160 (2003).
[29] M. M. Rogers and R. D. Moser, "Direct simulation of a self-similar turbulent mixing layer," Phys. Fluids **6**, 903–923 (1994).
[30] S. Ghosal and M. M. Rogers, "A numerical study of self-similarity in a turbulent plane wake using large-eddy simulation," Phys. Fluids **9**, 1729–1739 (1997).
[31] R. D. Moser, J. Kim, and N. N. Mansour, "Direct numerical simulation of turbulent channel flow up to $\mathrm{Re}_\tau = 590$," Phys. Fluids **11**, 943–945 (1999).
[32] P. Moin and J. Kim, "Numerical investigation of turbulent channel flow," J. Fluid Mech. **118**, 341–377 (1982).